

Dynamic Time Warping for Lead-Lag Relationships in Lagged Multi-Factor Models

Yichi Zhang^{1,4,*}, Mihai Cucuringu^{1,2,4,7}, Alexander Y. Shestopaloff^{5,6}, Stefan Zohren^{3,4,7}

¹*Department of Statistics, University of Oxford*

²*Mathematical Institute, University of Oxford*

³*Department of Engineering, University of Oxford*

⁴*Oxford-Man Institute of Quantitative Finance, University of Oxford*

⁵*School of Mathematical Sciences, Queen Mary University of London*

⁶*Department of Mathematics and Statistics, Memorial University of Newfoundland*

⁷*The Alan Turing Institute, London*

September 19, 2023

Abstract

In multivariate time series systems, lead-lag relationships reveal dependencies between time series when they are shifted in time relative to each other. Uncovering such relationships is valuable in downstream tasks, such as control, forecasting, and clustering. By understanding the temporal dependencies between different time series, one can better comprehend the complex interactions and patterns within the system. We develop a cluster-driven methodology based on dynamic time warping for robust detection of lead-lag relationships in lagged multi-factor models. We establish connections to the multireference alignment problem for both the homogeneous and heterogeneous settings. Since multivariate time series are ubiquitous in a wide range of domains, we demonstrate that our algorithm is able to robustly detect lead-lag relationships in financial markets, which can be subsequently leveraged in trading strategies with significant economic benefits.

Keywords: Dynamic Time Warping; High-dimensional time series; Lead-lag relationships; Unsupervised learning; Clustering; Financial markets

*Corresponding author; Email: yichi.zhang@stats.ox.ac.uk; The remaining authors are listed in alphabetical order.

Contents

1	INTRODUCTION	3
2	DYNAMIC TIME WARPING	4
3	Model setup	6
3.1	Description	7
4	Methodology	8
5	Synthetic data experiments	9
5.1	Synthetic data generating process	9
5.2	Simulation results	10
6	Financial data experiments	12
6.1	Data description	12
6.2	Data pre-processing	12
6.3	Benchmark	13
6.4	Trading strategies	13
6.5	Performance evaluation	14
6.6	Results	16
7	Robustness analysis	20
8	CONCLUSION AND FUTURE WORK	22
A	Appendix	26
A.1	Performance metrics	26
A.2	Synthetic data experiments	28
A.3	Futures data set details	30

1 INTRODUCTION

Natural physical systems often produce high-dimensional, nonlinear time series data, which are prevalent across various domains. Numerous contributions have been made to analyze such time series from different perspectives [Cao, Chen, and Hull (2020); Cartea, Donnelly, and Jaimungal (2018); Cont (2001); Cui, Yang, and Zhou (2021); Drinkall, Zohren, and Pierrehumbert (2022); Lu, Reinert, and Cucuringu (2022); Lu, Reinert, and Cucuringu (2023); Sokolov et al. (2022); Vuletić, Prenzel, and Cucuringu (2023); Álvaro Cartea (2023)]. For example, Cont (2001) explored financial time series and emphasized various statistical properties such as distributional characteristics, tail properties, and extreme fluctuations.

High-dimensional time series can offer valuable insights through the discovery of latent structures, such as lead-lag relationships. These relationships are commonly observed and play a significant role in the field of finance [Albers et al. (2021); Bennett, Cucuringu, and Reinert (2022); Buccheri, Corsi, and Peluso (2021); Ito and Sakemoto (2020); Y. Li et al. (2021); Miori and Cucuringu (2022); Tolikas (2018); Yao and H.-Y. Li (2020); Zhang, Cucuringu, A. Y. Shestopaloff, et al. (2023)], the environment De Luca and Pizzolante (2021); Wu et al. (2010), and biology Runge et al. (2019). For instance, Bennett, Cucuringu, and Reinert (2022) created a directed network to capture pairwise lead-lag relationships among equity prices in the US market. The analysis revealed clusters with significant directed flow imbalance.

Dynamic time warping (DTW) is an algorithm to quantify similarities between two time series, even when they exhibit variations in speed, enabling the calculation of an optimal alignment between them [Bellman and Kalaba (1959); Berndt and Clifford (1994); Keogh and Ratanamahatana (2005); Senin (2008)]. The versatility of DTW is evident in its application to diverse domains, such as financial markets [Gupta and Chatterjee (2020); Howard, Putninš, and Alexeev (2022); Ito and Sakemoto (2020); Stübinger and Walter (2022)], bioinformatics [Aach and Church (2001); Gavrilu, Davis, et al. (1995)], and robotics Schmill, Oates, and Cohen (1999). For example, Ito and Sakemoto (2020) introduced Multinomial Dynamic Time Warping (MDTW) to explore lead-lag relationships in FX market data. Howard, Putninš, and Alexeev (2022) applied DTW and found that global market price discovery oscillates between S&P 500 futures and FTSE 100 futures. Despite the widely recognized importance and potentially high impact of the problem, limited progress has been made in robustly using DTW for the inference of lead-lag relationships in lagged multi-factor models.

Summary of main contributions.

1. We introduce a computationally scalable framework for lead-lag detection in high-dimensional time series based on DTW, with clustering used as a denoising step.
2. We show it is capable of reliably detecting lead-lag relationships in a variety of factor model-based simulated high-dimensional time series.
3. In financial markets, we leverage the detected lead-lag relationships to construct a profitable trading strategy and demonstrate that our algorithm outperforms the benchmark in most cases.
4. Our algorithm is also faster than the benchmark in terms of computing time by a factor of 10.

Paper outline. This paper is organized as follows. Section 2 and Section 3 introduce the definition of DTW and the *lagged multi-factor model*. Section 4 describes our proposed DTW algorithm. In Section 5, we validate our algorithm on synthetic data sets from the lagged multi-factor model, and explore lead-lag relationships in the US equity, ETF, and futures markets in Section 6. We then move on to a robustness analysis in Section 7. Finally, we summarize our findings, and discuss possible future research directions in Section 8.

2 DYNAMIC TIME WARPING

In this section, we introduce the DTW algorithm. Suppose we have two time series, denoted as A and B with lengths n and m , respectively, shown in Figure 1 Step 1.

$$\begin{aligned} A &= a_1, a_2, \dots, a_i, \dots, a_n \\ B &= b_1, b_2, \dots, b_j, \dots, b_m \end{aligned} \tag{1}$$

In order to align two time series utilizing DTW, the process involves constructing an $n \times m$ matrix, where the $(i^{\text{th}}, j^{\text{th}})$ element of the matrix contains the Euclidean distance $d(a_i, b_j)$ between the two points a_i and b_j from A and B , respectively, i.e. $d(a_i, b_j) = (a_i - b_j)^2$. Each matrix element (i, j) corresponds to the alignment between the points a_i and b_j . Figure 1 Step 2 illustrates an example of the distance matrix.

A warping path, denoted as W , represents a consecutive set of matrix elements that capture the mapping between time series A and B . The index of the DTW can be expressed as follows

$$W = \{w_1, w_2, \dots, w_k, \dots, w_K\} \quad \max(m, n) \leq K < m + n - 1 \tag{2}$$

where the k^{th} element of W is denoted as $w_k = (i, j)_k$.

The warping path must adhere to several constraints:

- **Boundary:** The warping path starts at $w_1 = (1, 1)$ and ends at $w_K = (m, n)$. This ensures that the warping path initiates from the bottom-left corner cell and terminates at the top-

right corner cell of the matrix.

- **Continuity:** For a given $w_k = (x, y)$, the preceding element $w_{k-1} = (x', y')$, where $x - x' \leq 1$ and $y - y' \leq 1$. This restriction allows only adjacent cell transitions within the warping path.
- **Monotonicity:** For a given $w_k = (x, y)$, the preceding element $w_{k-1} = (x', y')$, where $x - x' \geq 0$ and $y - y' \geq 0$. This constraint ensures that the points in W exhibit monotonically increasing indices over time.

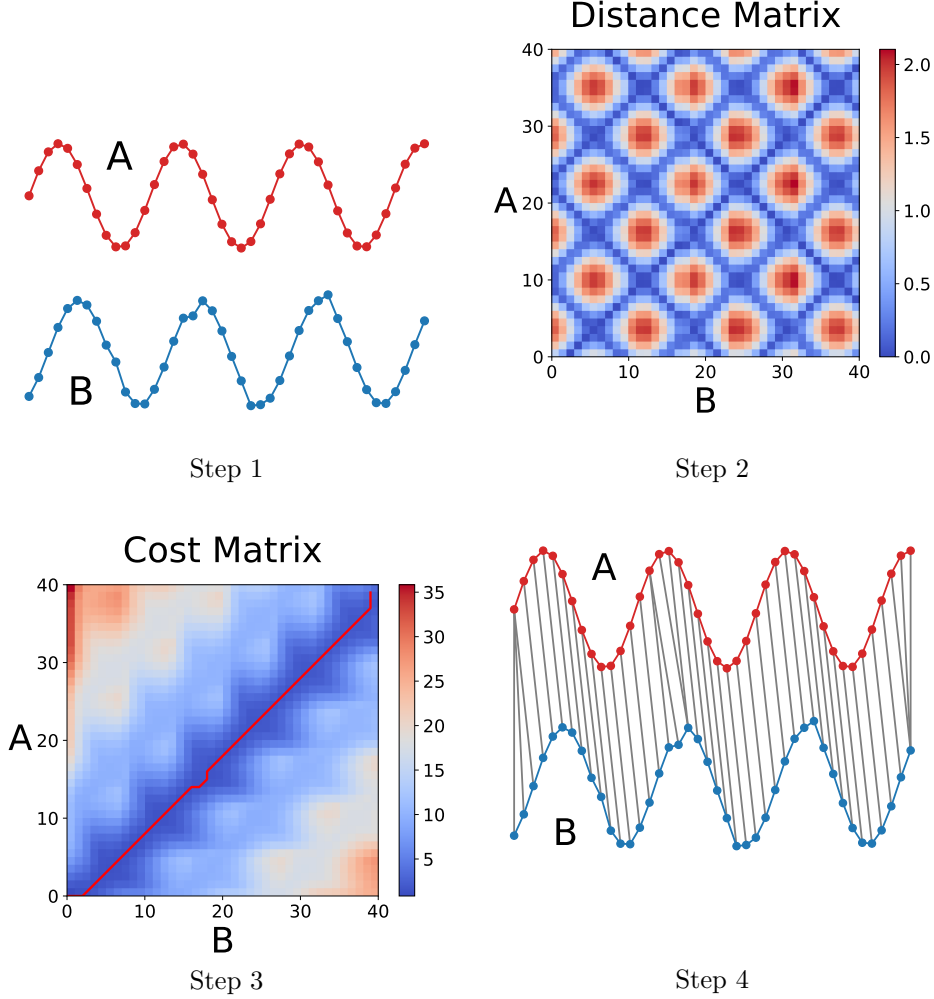


Figure 1: Step 1: Two time series A and B are similar, but they are out of phase with each other. Step 2: The distance matrix, which the $(i^{\text{th}}, j^{\text{th}})$ element of the matrix has the value of the Euclidean distance $d(a_i, b_j)$ from A and B , respectively. Step 3: The cost matrix, which contains the optimal warping path, is visually indicated by the red line. Step 4: The resulting alignment between the two time series, A and B , is shown.

Among the various warping paths that adhere to the aforementioned constraints, our objective is to identify the path that minimizes the warping cost

$$\text{DTW}(A, B) = \min \left\{ \sqrt{\sum_{k=1}^K w_k} \right\}. \quad (3)$$

To find this optimal path, dynamic programming techniques are employed to evaluate the following subsequent recurrence relation, which defines the cumulative distance $c(i, j)$ as the distance $d(i, j)$ located in the current cell as well as the minimum of the cumulative distances of the adjacent

elements

$$c(i, j) = d(a_i, b_j) + \min\{c(i-1, j-1), c(i-1, j), c(i, j-1)\} \quad (4)$$

In Figure 1 Step 3, the optimal path is depicted by a red line. The resulting alignment can be seen in Figure 1 Step 4. In conclusion, the complete DTW algorithm is illustrated below

Algorithm 1 Dynamic Time Warping (DTW)

Input: Time series A with length n , time series B with length m .

```

1: procedure DTW( $A$  : array [1.. $n$ ],  $B$  : array [1.. $m$ ])
2:    $DTW \leftarrow$  array [0.. $n$ , 0.. $m$ ]
3:   for  $i \leftarrow 0$  to  $n$  do
4:     for  $j \leftarrow 0$  to  $m$  do
5:        $DTW[i, j] \leftarrow \infty$ 
6:    $DTW[0, 0] \leftarrow 0$ 
7:   for  $i \leftarrow 1$  to  $n$  do
8:     for  $j \leftarrow 1$  to  $m$  do
9:        $cost \leftarrow d(A[i], B[j])$ 
10:       $DTW[i, j] \leftarrow cost + \min(DTW[i-1, j],$ 
11:         $DTW[i, j-1], DTW[i-1, j-1])$ 
12:   return  $DTW[n, m]$ 

```

Note that the Euclidean distance between two time series can be considered as a specific case of DTW, where the warping path W is constrained such that $w_k = (i, j)_k$ with $i = j = k$. In other words, the window size S is set to 0. This constraint is applicable only when the two time series have the same length. A visual comparison of the Euclidean distance and DTW is presented in Figure 2.

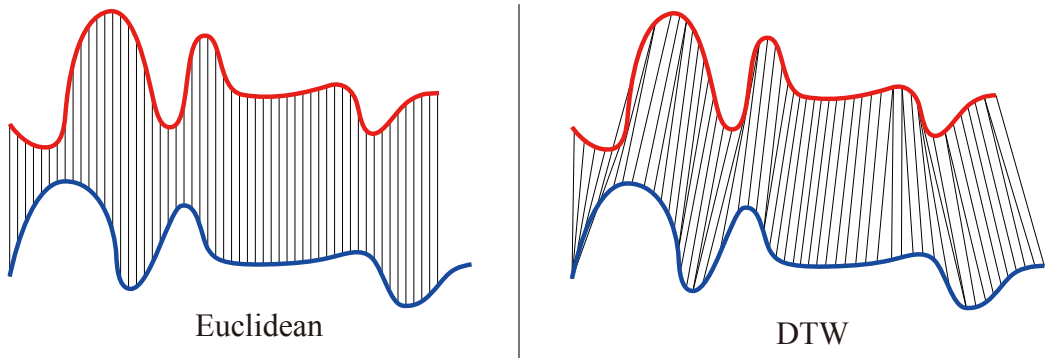


Figure 2: Left: Euclidean distance measures direct the i^{th} point in one time series aligns with the i^{th} point in another time series, assuming the same length, which will yield a pessimistic dissimilarity measure. Right: DTW accounts for variations in speed and calculates optimal alignment between two time series, allowing for different lengths, which is more flexible in calculating the intuitive distance measure.

3 Model setup

In this section, we will introduce both the standard and lagged versions of the *multi-factor model*, which we will adopt as the underlying model for our time series data. Specifically, we will employ the lagged multi-factor model to validate our algorithm using synthetic data before applying it to real-world scenarios. The fundamental idea behind these models is to represent a time series as a

(noisy) combination of factors, with each factor exhibiting different levels of exposure. The model we propose for the detection of lead-lag relationships exhibits significant parallels with the problem of multireference alignment (MRA), which is concerned with the estimation of a single signal from a set of n cyclically and noisily shifted copies of itself, as shown in Bandeira et al. (2014).

3.1 Description

Let us begin by revisiting the standard multi-factor model for a multivariate time series

$$X_i^t = \sum_{j=1}^k B_{ij} f_j^t + \epsilon_i^t \quad i = 1, \dots, n; \quad t = 1, \dots, T, \quad (5)$$

where X_i^t is the time series i (e.g., the excess return of a financial asset) at time t , k is the number of factors, B_{ij} is the exposure of time series i to factor j , f_j^t is the factor j at time t , and ϵ_i^t is the noise at time t , with variance σ^2 . Furthermore, we have n as the total number of time series, and T as the total number of time steps.

In this paper, our emphasis is on the lagged version of the multi-factor model, which can be expressed as follows

$$X_i^t = \sum_{j=1}^k B_{ij} f_j^{t-L_{ij}} + \epsilon_i^t \quad i = 1, \dots, n; \quad t = 1, \dots, T, \quad (6)$$

where the primary distinction in the lagged multi-factor model, in comparison to the standard multi-factor model, is the inclusion of L_{ij} , representing the lag at which time series i is exposed to factor j . Consequently, $f_j^{t-L_{ij}}$ corresponds to the value of factor j at time $t - L_{ij}$.

In the lagged multi-factor model (6), we consider two key settings, which are first introduced in Zhang, Cucuringu, A. Y. Shestopaloff, et al. (2023)

- **Single Membership:** Each time series has a lagged exposure to a single factor. We consider the following two main categories.
 - **Homogeneous Setting:** The model only has one factor, i.e. $k = 1$.
 - **Heterogeneous Setting:** The model has more than one factor, i.e. $k \geq 2$. However, each time series is exposed only to a single factor.
- **Mixed Membership:** Each time series is permitted to have a lagged exposure to more than one factor, resulting in a mixed configuration. Therefore, the model comprises at least two factors, indicated by $k \geq 2$.

In this paper, our primary objective is to perform inference on the lag values L_{ij} in the lagged multi-factor model, specifically focusing on the single membership setting. We do not place emphasis on the inference of the unknown coefficient matrix B and factors f . As shown later, the estimation of L_{ij} alone holds practical significance in specific applications, such as finance. The investigation of the mixed membership setting is left for future work.

4 Methodology

In this section, we propose a robust algorithm for detecting lead-lag relationships using the combination of DTW and K-Medoids (DTW_KMed), and use the DTW library from Meert et al. (2020).

We consider a set of time series denoted as $X_{n \times T}$ as our input. Initially, we employ DTW to compute pairwise distances between every pair of time series from $X_{n \times T}$. Subsequently, we apply K-Medoids clustering to group similar time series into clusters based on the DTW distance matrix. The pairs of time series i and j are denoted as $\{X_i, X_j\}$. For each cluster ϕ_d ($d = 1, \dots, K$), we record the path $W\{X_i, X_j\}$ by performing DTW on $\{X_i, X_j\}$. Then, we calculate the difference for each index pair in the path W , denoted as $\Delta(W\{X_i, X_j\})$. The calculation can be expressed as follows

$$\Delta(W\{X_i, X_j\}) = \{\Delta(w_1), \Delta(w_2), \dots, \Delta(w_k), \dots, \Delta(w_K)\} \quad (7)$$

where $\max(m, n) \leq K < m + n - 1$, and $\Delta(w_K) = \Delta((i, j)_k) = i - j$.

Then, the value of relative lags of $\{X_i, X_j\}$ in ϕ_d (estimated by mode or median) can be expressed as

$$\gamma\{X_i, X_j\} = \begin{cases} \text{Mode}(\Delta(W\{X_i, X_j\})) & \text{Mode estimation} \\ \text{Median}(\Delta(W\{X_i, X_j\})) & \text{Median estimation} \end{cases} \quad (8)$$

For instance, once we have applied K-medoids clustering using the DTW distance matrix computed from $X_{n \times T}$, let's consider two time series, X_1 and X_2 , that contain 100 data points and belong to the same cluster, with a known ground truth lag value of 3. Subsequently, we calculate the relative lags of $\Delta(W\{X_1, X_2\})$. Figure 3 illustrates the relative lags obtained from $\{X_1, X_2\}$.

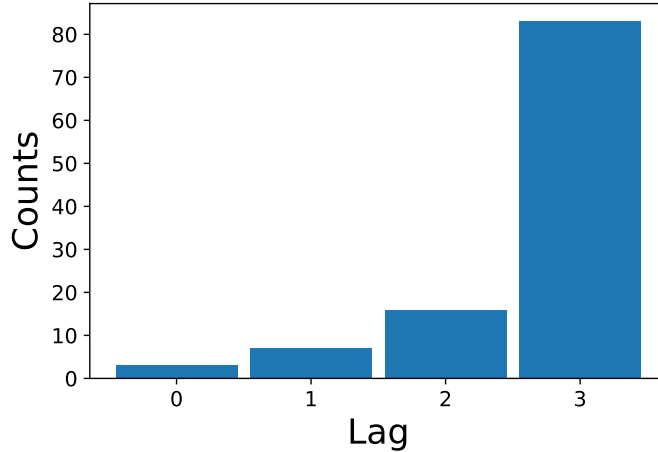


Figure 3: Histogram of the relative lags from two time series.

By employing mode or median estimation of $\Delta(W\{X_1, X_2\})$, denoted as $\gamma\{X_1, X_2\}$, with a value of 3, as evident from Figure 3, we can conclude that the result remains consistent and robust with respect to the ground truth value. Despite the presence of outliers, such as $\{0, 1, 2\}$, in $\Delta(W\{X_i, X_j\})$, the estimated lag value aligns well with the ground truth value of 3.

Next step, the construction of the lead-lag matrix $\Gamma_{n \times n}$ is accomplished by

$$\Gamma_{ij} = \begin{cases} \gamma\{X_i, X_j\} & \text{if } X_i \text{ and } X_j \text{ are in the same cluster} \\ 0 & \text{otherwise} \end{cases} \quad (9)$$

We summarize the above procedures in Algorithm 2.

Algorithm 2 DTW_KMed for Lead-lag Relationship Detection

Input: Time series matrix $X_{n \times T}$. **Output:** Lead-lag matrix $\Gamma_{n \times n}$.

- 1: Compute the DTW distance matrix from $X_{n \times T}$.
 - 2: Apply K-medoids clustering using the DTW distance matrix.
 - 3: For each cluster ϕ_d ($d = 1, \dots, K$):
 - Record path W from every pair of time series $\{X_i, X_j\}$.
 - Calculate the difference $\Delta(W\{X_i, X_j\})$ for every index pair in the path W
 - Record lag $\gamma\{X_i, X_j\}$ by taking *mode* or *median* estimation of the difference $\Delta(W\{X_i, X_j\})$.
 - 4: Calculate the lead-lag matrix $\Gamma_{n \times n}$ by setting $\gamma\{X_i, X_j\}$, where $\{X_i, X_j\}$ is in the same cluster. Otherwise, the entry is set to 0.
-

5 Synthetic data experiments

The synthetic data experiments serve the purpose of simulating data generated by a multi-factor model with a known ground truth lead-lag matrix L . The main objective is to evaluate and validate the performance of our proposed algorithms under various scenarios.

5.1 Synthetic data generating process

As noted earlier, our focus is the single membership setting. We generate synthetic data from the lagged multi-factor model (6) with $k = \{1, 2\}$ factors. Furthermore, we specify the maximum number of lags as $M = 5$ and the length of the time series as $T = 100$. The factors f and noise ϵ are drawn from $\mathcal{N}(0, 1)$. We define B and L as follows:

Table 1: Top row: Loading matrix B . Bottom row: Lag matrix L .

	Homogeneous Setting	Heterogeneous Setting	
B	$\begin{bmatrix} 1 \\ 1 \\ 1 \\ 1 \\ 1 \\ 1 \end{bmatrix}$	$\begin{bmatrix} 1 & 0 \\ 1 & 0 \\ 1 & 0 \\ 0 & 1 \\ 0 & 1 \\ 0 & 1 \end{bmatrix}$	$\begin{bmatrix} 1 & 0 & 0 \\ 1 & 0 & 0 \\ 0 & 1 & 0 \\ 0 & 1 & 0 \\ 0 & 0 & 1 \\ 0 & 0 & 1 \end{bmatrix}$
L	$\begin{bmatrix} 0 \\ 1 \\ 2 \\ 3 \\ 4 \\ 5 \end{bmatrix}$	$\begin{bmatrix} 0 & 0 \\ 2 & 0 \\ 4 & 0 \\ 0 & 0 \\ 0 & 2 \\ 0 & 4 \end{bmatrix}$	$\begin{bmatrix} 0 & 0 & 0 \\ 3 & 0 & 0 \\ 0 & 0 & 0 \\ 0 & 3 & 0 \\ 0 & 0 & 0 \\ 0 & 0 & 3 \end{bmatrix}$
	$k = 1$	$k = 2$	$k = 3$

For validation purposes, we set the number of time series as $n = 120$ to demonstrate the

effectiveness of our algorithms. When estimating the lead-lag matrix, we use a sliding window of length $l = 21$ and a shift of $s = 1$. After estimating the lead-lag matrix, we calculate the error matrix E to evaluate the performance, which we denote as

$$E_{n \times n} = \Gamma_{n \times n} - \Psi_{n \times n}, \quad (10)$$

where $\Gamma_{n \times n}$ is the estimated lead-lag matrix, and $\Psi_{n \times n}$ is the ground truth lead-lag matrix, which can be obtained from $L_{n \times k}$.

5.2 Simulation results

In the homogeneous setting ($k = 1$), as shown in Figure 4, all five algorithms (KM as K-Means, Euc_KMed as Euclidean + K-Medoids, Man_KMed as Manhattan + K-Medoids, Cos_KMed as Cosine + K-Medoids, and DTW_KMed as DTW + K-Medoids) demonstrate optimal performance with an Adjusted Rand Index (ARI) of 1. This indicates that they successfully detect the lead-lag relationships with high accuracy when there is only one underlying factor, and this result is expected based on our experimental setup. However, in the heterogeneous setting ($k = 2$), we observe a general decrease in ARI as the noise level σ increases. Despite this trend, our proposed DTW_KMed algorithm achieves a consistently high ARI value within the range of σ from 0 to 1.5. This performance surpasses the other algorithms, which maintain relatively lower ARI values across the noise levels. This observation highlights that DTW excels in capturing intricate lead-lag patterns with a higher level of robustness.

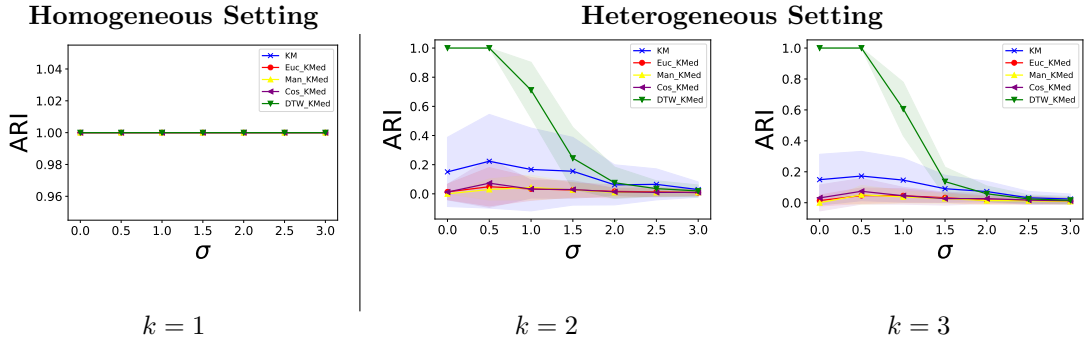


Figure 4: Average and confidence interval for the ARI with different σ levels based on 100 simulations for every iteration.

In DTW, the window size S defines the maximum allowed shifts from the two diagonals smaller than this number. Hence, selecting the appropriate window size S is of critical importance in DTW. The choice of S affects how much temporal distortion is allowed between time series, thereby influencing the alignment and capturing the underlying lead-lag relationships effectively. Properly tuning S enables DTW to strike a balance between capturing complex patterns while avoiding excessive warping that might lead to misclassification.

Across the synthetic experiments, we set the true lag equal to 5. In Figure 5, we observe similar results to the homogeneous setting in Figure 4. However, in the heterogeneous setting, the ARI tends to be relatively lower when the window size ranges from 0 to 5. Conversely, when the window size equals or exceeds 5, the ARI increases significantly.

This behaviour aligns with the rationale that DTW requires a window size that equals or exceeds the true lag of 5. This enables DTW to calculate the optimal alignment with enough flexibility to capture the actual lead-lag relationship effectively. When the window size is too restrictive, it may not allow for sufficient temporal distortion, leading to suboptimal alignment and lower ARI values in the presence of multiple factors. As such, selecting an appropriate window size is crucial to ensure accurate lead-lag relationship detection with DTW.

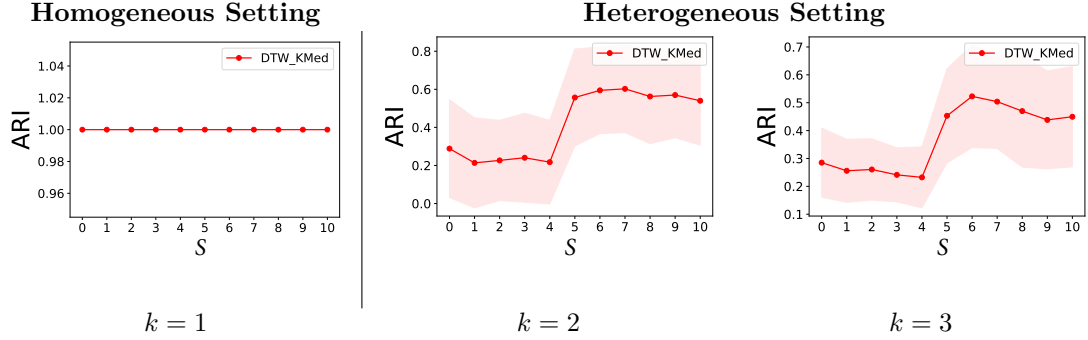


Figure 5: Average and confidence interval for the ARI with different window sizes S based on 100 simulations for every iteration (the true lag is 5).

As depicted in Figure 6, for both the homogeneous and heterogeneous settings, the Mean Squared Error (MSE) remains close to 0 when σ ranges from 0.0 to 0.5. However, as σ increases beyond 0.5, the MSE rises significantly for both algorithms. Overall, both algorithms demonstrate acceptable performance for low noise levels, but the DTW_KMed mode estimation (DTW_KMed_Mod) exhibits better performance across varying levels of noise than DTW_KMed median estimation (DTW_KMed_Med).

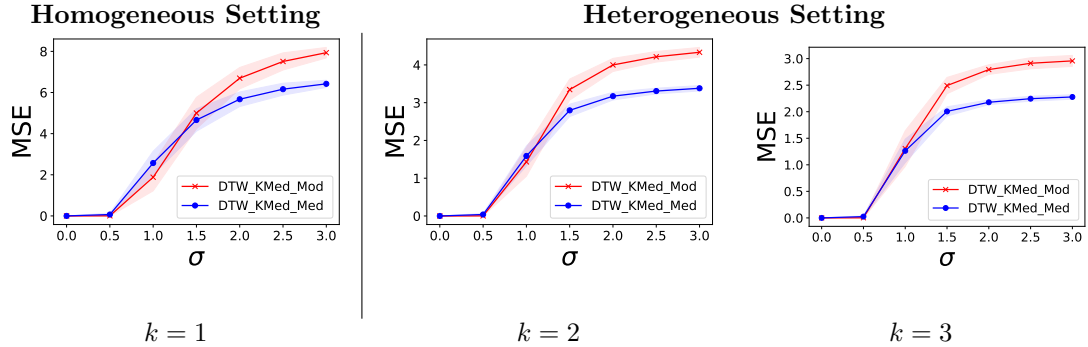


Figure 6: Average and confidence interval for the MSE with different σ levels based on 100 simulations for every iteration.

With the true lag set as 5 and σ as 1, the DTW_KMed_Mod algorithm outperforms the DTW_KMed_Med algorithm in the homogeneous setting ($k = 1$). In the heterogeneous setting ($k = 2$), when the window size S ranges from 0 to 5, the MSE is higher for both algorithms. However, as the window size S exceeds 5, both algorithms achieve a lower MSE. This behaviour aligns with the understanding that DTW requires a S that equals or exceeds the true lag of 5 to effectively calculate the optimal alignment. Thus, when the S is less than 5, the alignment may not fully capture the true lead-lag relationship, resulting in higher MSE values. However, when the S is larger than or equal to 5, both algorithms achieve better alignment, leading to reduced

MSE values.

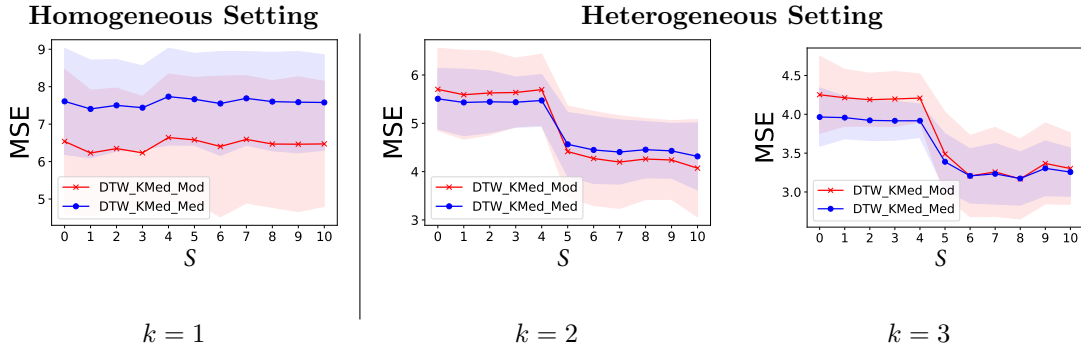


Figure 7: Average and confidence interval for the MSE with different window sizes S based on 100 simulations for every iteration (the true lag is 5, and σ is 1).

6 Financial data experiments

6.1 Data description

In this section, we conduct a large-scale experiment using financial data to apply our algorithms. As mentioned earlier, this is a context where lead-lag relationships naturally occur. For our financial data experiments, we consider three different data sets, each varying in terms of the number and type of assets, as well as the number of days included in the data set. All the data sets are considered at a daily frequency. The summarized details of the data sets are presented in Table 2, with additional information about the Pinnacle Data Corp CLC data set available in the Appendix A.3 Tables [12, 13, 14, 19, 15, 16, 17, 18].

Table 2: Summary of the three financial data sets considered in the numerical experiments.

Data source	Type	Freq	# of assets	Start date	End date	# of days
Wharton’s CRSP	Equity	Daily	679	2000/01/03	2019/12/31	5211
Wharton’s CRSP	ETF	Daily	14	2006/04/12	2019/07/01	3324
Pinnacle Data Corp	Futures	Daily	52	2000/01/05	2020/10/16	5166

6.2 Data pre-processing

With regard to the US equity and ETF data sets, we use the close-to-close adjusted daily returns from Wharton’s CRSP. Due to the large number of NaNs in the equity data set, we drop the days for which more than 10% of the equities have zero returns as well as the equities for which more than 50% of days have zero returns. Instead of working with raw returns, we consider the *market excess returns*, a standard measure of how well each equity performed relative to the broader market. For both of these data sets, the return of the S&P Composite Index is selected to compute the market excess returns by subtracting it from the return of each asset (i.e., for simplicity, we assume each asset has $\beta = 1$ exposure to the market). Also, we winsorize the extreme value of excess returns for which any value is larger than 0.15 or smaller than -0.15.

For the futures data set, we use the close-to-close price series from the Pinnacle Data Corp CLC data set, and discard the days for which more than 10% of the futures have zero prices in the respective dates, and drop the futures for which more than 160 days have zero prices. Afterwards, we first use forward-fill, then backward-fill to fill out the zero prices. Lastly, we compute the log-return from the close-to-close price. The remainder of the data pre-processing is the same as above.

6.3 Benchmark

In order to evaluate our proposed methodology, we also introduce a benchmark to detect lead-lag relationships without the use of clustering. It is very common to compute a sample cross-correlation function (CCF) between two time series. A CCF between time series X_i and X_j evaluated at lag m is given by

$$\text{CCF}^{ij}(m) = \text{CORR}(\{X_i^{t-m}\}, \{X_j^t\}), \quad (11)$$

where $\text{CORR}()$ denotes a choice of the CCF. The corresponding lead-lag matrix $\Gamma_{n \times n}$ is estimated by computing the signed normalized area under the curve of CCF, given by

$$\Gamma_{ij} = \frac{\text{MAX}(I(i, j), I(j, i)) \cdot \text{SIGN}(I(i, j) - I(j, i))}{I(i, j) + I(j, i)}, \quad (12)$$

where $I(i, j) = \sum_{m=1}^M |\text{CCF}^{ij}(m)|$ for a user-specified maximum lag M .

We summarize the CCF procedures in Algorithm 3.

Algorithm 3 : CCF Algorithm

Input: Time series matrix $X_{n \times T}$.

Output: Lead-lag matrix $\Gamma_{n \times n}$.

- 1: Calculate CCF for every pair of time series $\{X_i, X_j\}$.
 - 2: Calculate the lead-lag matrix $\Gamma_{n \times n}$ by computing the signed normalized area under the curve of CCF.
-

Also, we use four algorithms (KM_Mod, KM_Med, SP_Mod, and SP_Med) as our benchmark from Zhang, Cucuringu, A. Y. Shestopaloff, et al. (2023).

6.4 Trading strategies

In this section, we present the trading strategies employed in this paper. Our approach involves a series of steps applied to a dataset consisting of n time series, each having a length of T . Firstly, we extract the data by implementing a sliding window approach with a fixed length of $l = 21$. Subsequently, we employ the DTW_KMed algorithm to detect the lead-lag relationship, which is further validated through a synthetic data experiment. Once the lead-lag matrix is obtained, We then utilize the lead-lag matrix to rank the time series from the most leading to the most lagging using the *RowSum* ranking [Gleich and L.-h. Lim (2011); Huber (1963)], in order to then group the time series into leaders and laggards, where the leaders are employed to forecast the behaviour of the laggards.

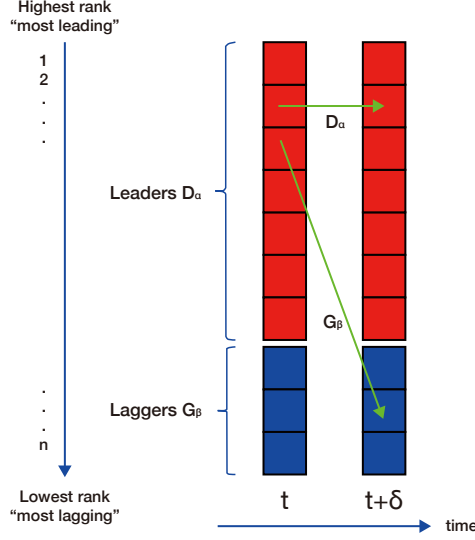


Figure 8: G_β strategy: Use D_α predict G_β . D_α strategy: Use D_α predict D_α .

Momentum, a well-studied phenomenon in finance literature [Jegadeesh, Luo, et al. (2022); Jegadeesh and Titman (2001); B. Lim, Zohren, and Roberts (2019); Poh, Roberts, and Zohren (2022); Tan, Roberts, and Zohren (2023); Wood, Giegerich, et al. (2021); Wood, Roberts, and Zohren (2021); Roberts, Dong, Zohren, et al. (2023); Zohren, Roberts, Dong, et al. (2023)], refers to the tendency of assets that have exhibited strong performance in the recent past to continue their performance in the near future, and vice versa. In our trading strategy, we identify the top $\alpha = 0.75$ fraction of the time series as Leaders D_α , while the remaining bottom fraction $\beta = 1 - \alpha$ is classified as Laggers G_β . To predict the future performance, we employ the exponentially weighted moving average (EWMA) signal, considering the past $p = \{1, 3, 5, 7\}$ days of average winsorized time series excess returns from D_α . This prediction aims to estimate the average excess returns of G_β and D_α in the subsequent $\delta = \{1, 3, 5, 7\}$ days. We assume that G_β can catch up with D_α , while D_α provides the necessary momentum to sustain the trend over the δ days. Figure 8 visually illustrates this concept. To ensure continuous trading, we shift the sliding window by $h = 1$ and repeat the lead-lag matrix calculation and ranking steps until the end of the time series. Figure 9 provides a depiction of our trading pipeline at time t , and we summarize the trading strategy in Algorithm 4.

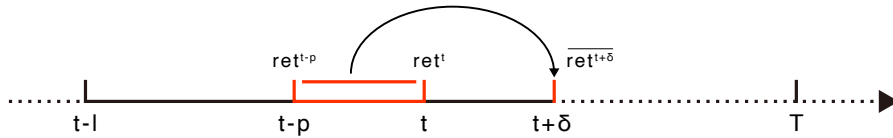


Figure 9: Illustration of the trading pipeline at time t , given the EWMA of past p days of average winsorized time series excess returns to predict future δ days average excess returns.

6.5 Performance evaluation

When assessing the effectiveness of various trading strategies, we rely on the following metrics to evaluate their performance. We compute the Profit and Loss (PnL) of G_β on a given day $t + \delta$ as

Algorithm 4 : Trading strategy

Input: Time series matrix $X_{n \times T}$.

- 1: Construct the matrix $X_{n \times T}$ by employing a sliding window of length l starting from the beginning of the time series, resulting in $X_{n \times l}$.
 - 2: Apply the **DTW_KMed for Lead-lag Relationship Detection Algorithm** to $X_{n \times l}$, resulting in the computation of the lead-lag matrix $\Gamma_{n \times n}$.
 - 3: Based on $\Gamma_{n \times n}$, rank the time series from the most leading to the most lagging using the *RowSum* ranking methodology.
 - 4: Select the top α fraction of the time series as Leaders D_α , and the bottom $\beta = 1 - \alpha$ as Laggards G_β .
 - 5: Employ the Exponentially Weighted Moving Average (EWMA) on the past p days of the average winsorized time series excess returns of D_α to predict the average future excess returns of G_β and D_α for a duration of δ days.
 - 6: Shift the sliding window by h , and repeat Steps 1-5 until the end of the time series.
-

$$\text{PnL}_{G_\beta}^{t+\delta} = \text{sign}(\text{EWMA}(\text{ret}_{D_\alpha}^{t-p} : \text{ret}_{D_\alpha}^t)) \cdot \overline{\text{ret}_{G_\beta}^{t+\delta}}, t = l, \dots, T - \delta, \quad (13)$$

since the strategy makes profits whenever the sign of the forecast agrees with the sign of the future return. Correspondingly, the PnL of D_α on a given day $t + \delta$ is given by

$$\text{PnL}_{D_\alpha}^{t+\delta} = \text{sign}(\text{EWMA}(\text{ret}_{D_\alpha}^{t-p} : \text{ret}_{D_\alpha}^t)) \cdot \overline{\text{ret}_{D_\alpha}^{t+\delta}}, t = l, \dots, T - \delta, \quad (14)$$

where $\text{ret}_{D_\alpha}^{t-p}$ and $\text{ret}_{D_\alpha}^t$ are the excess return of D_α at $t-p$ and t , respectively, while $\text{EWMA}(\text{ret}_{D_\alpha}^{t-p} : \text{ret}_{D_\alpha}^t)$ denotes the exponentially weighted moving average from the excess return of D_α from $t-p$ to t . Furthermore, $\overline{\text{ret}_{G_\beta}^{t+\delta}}$ depicts the mean of the excess return of G_β at $t + \delta$, and $\overline{\text{ret}_{D_\alpha}^{t+\delta}}$ is the mean of the excess return of D_α at $t + \delta$.

We rescale the PnL by their volatility to target equal risk assignment, and set our annualized volatility target σ_{tgt} to be 0.15.

$$\text{PnL}_{\text{rescaled}} = \frac{\sigma_{\text{target}}}{\text{STD}(\text{PnL}) \cdot \sqrt{252}} \cdot \text{PnL}. \quad (15)$$

Based on $\text{PnL}_{\text{rescaled}}$, we proceed to calculate the following annualized metrics, in line with the works of [B. Lim, Zohren, and Roberts (2019); Wood, Roberts, and Zohren (2022); Tan, Roberts, and Zohren (2023); Poh, Roberts, and Zohren (2022); Wood, Giegerich, et al. (2021); Wood, Roberts, and Zohren (2021); Zhang, Cucuringu, A. Y. Shestopaloff, et al. (2023); Liu and Zohren (2023); Liu, Roberts, and Zohren (2023)], and more detailed information can be found in the Appendix A.1.

- **Profitability:** cumulative PnL, annualized expected excess return (E>Returns]), hit rate.
- **Risk:** volatility, downside deviation, maximum drawdown.
- **Performance:** Sortino ratio, Calmar ratio, average profit / average loss, PnL per trade, Sharpe ratio, P-value.

6.6 Results

In the case of the equity data set, comprehensive results with various tuning settings are available in Supplemental material [Zhang, Cucuringu, A. Shestopaloff, et al. (2023)] B.1. Our findings indicate that utilizing the EWMA on the past seven days of the average winsorized time series excess returns of the D_α , with $\alpha = 0.75$, for predicting the average future seven days of the excess return of the G_β and D_α consistently yields favourable performance across all algorithms. Figure 10 presents a comparison of cumulative PnL for the G_β strategy (left) and D_α strategy (right). In the G_β strategy, before 2008, the Sharpe ratio (SR) of DTW_KMed_Mod and DTW_KMed_Med outperformed the other algorithms. However, after 2008, except for CCF, all algorithms displayed a substantial growth trend and eventually achieved similar performance levels. On the other hand, in the D_α strategy, before 2008, all algorithms performed at roughly the same level. However, after 2008, DTW_KMed_Med emerged as the most profitable strategy, clearly outperforming others with an SR of 0.93. Additionally, Tables [3, 4] present the performance of DTW_KMed_Mod, DTW_KMed_Med, and other algorithms for the G_β strategy and D_α strategy based on various metrics (rescaled to target volatility).

Tables [5, 6] along with Figure 11 present the results for the ETF data set using the same settings as for the equity data. In the G_β strategy, we do not find evidence of consistently detecting lead-lag relationships that lead to a profitable outcome. However, in the D_α strategy, the SR of SP_Med and DTW_KMed_Mod are leading with SR values of 0.8 and 0.78, respectively. Full results across all tuning settings are reported in Supplemental material [Zhang, Cucuringu, A. Shestopaloff, et al. (2023)] B.2.

Results for the futures data, using the same settings as for the equity data, are presented in Tables [7, 8], along with Figure 12. For this data set, we do not observe the ability to consistently detect profitable lead-lag relationships for any of the strategies. Full results across all tuning settings are available in Supplemental material [Zhang, Cucuringu, A. Shestopaloff, et al. (2023)] B.3.

In addition to the real data results, we have also included the results of the synthetic data experiments in the Appendix A.2.

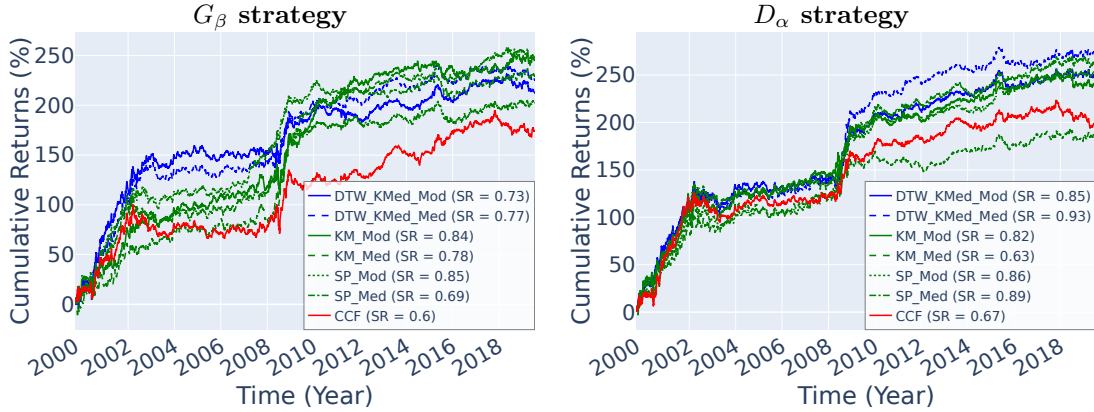


Figure 10: Equity data set: cumulative PnL for G_β strategy (left) and D_α strategy (right) - rescaled to target volatility. The experiment has been set with the values $p = 7$, $\delta = 7$, $\alpha = 0.25$, and $K = 5$.

G_β strategy	Benchmark					Proposed	
	CCF	KM_Mod	KM_Med	SP_Mod	SP_Med	DTW_KMod_Mod	DTW_KMod_Med
E[Returns]	0.089	0.126	0.118	0.127*	0.104	0.109	0.115
Volatility	0.15	0.15	0.15	0.15	0.15	0.15	0.15
Downside deviation	0.105	0.103	0.101*	0.103	0.105	0.106	0.107
Maximum drawdown	-0.313	-0.26	-0.215	-0.214	-0.287	-0.205	-0.188*
Sortino ratio	0.85	1.222	1.166	1.237*	0.988	1.026	1.084
Calmar ratio	0.285	0.484	0.548	0.594	0.362	0.531	0.614*
Hit rate	0.499	0.521*	0.51	0.516	0.519	0.514	0.512
Avg. profit / avg. loss	1.117*	1.068	1.107	1.091	1.051	1.08	1.1
PnL per trade	3.542	4.996	4.672	5.041*	4.119	4.317	4.581
Sharpe ratio	0.595	0.839	0.785	0.847*	0.692	0.725	0.77
P-value	0.009	0*	0*	0*	0.002	0.001	0.001

Table 3: Equity data set: performance metrics for G_β strategy - rescaled to target volatility. The experiment has been set with the values $p = 7$, $\delta = 7$, $\alpha = 0.25$, and $K = 5$.

G_β strategy	Benchmark					Proposed	
	CCF	KM_Mod	KM_Med	SP_Mod	SP_Med	DTW_KMod_Mod	DTW_KMod_Med
E[Returns]	0.101	0.122	0.095	0.129	0.134	0.128	0.14*
Volatility	0.15	0.15	0.15	0.15	0.15	0.15	0.15
Downside deviation	0.105	0.107	0.108	0.106	0.105	0.103	0.102*
Maximum drawdown	-0.288	-0.251	-0.21*	-0.283	-0.227	-0.276	-0.297
Sortino ratio	0.964	1.148	0.876	1.222	1.269	1.238	1.376*
Calmar ratio	0.352	0.488	0.452	0.456	0.59*	0.463	0.472
Hit rate	0.518	0.521	0.513	0.522	0.525*	0.52	0.523
Avg. profit / avg. loss	1.05	1.069	1.066	1.072	1.065	1.078*	1.078*
PnL per trade	4.018	4.856	3.765	5.121	5.312	5.073	5.557*
Sharpe ratio	0.675	0.816	0.632	0.86	0.892	0.852	0.934*
P-value	0.003	0*	0.005	0*	0*	0*	0*

Table 4: Equity data set: performance metrics for D_α strategy - rescaled to target volatility. The experiment has been set with the values $p = 7$, $\delta = 7$, $\alpha = 0.25$, and $K = 5$.

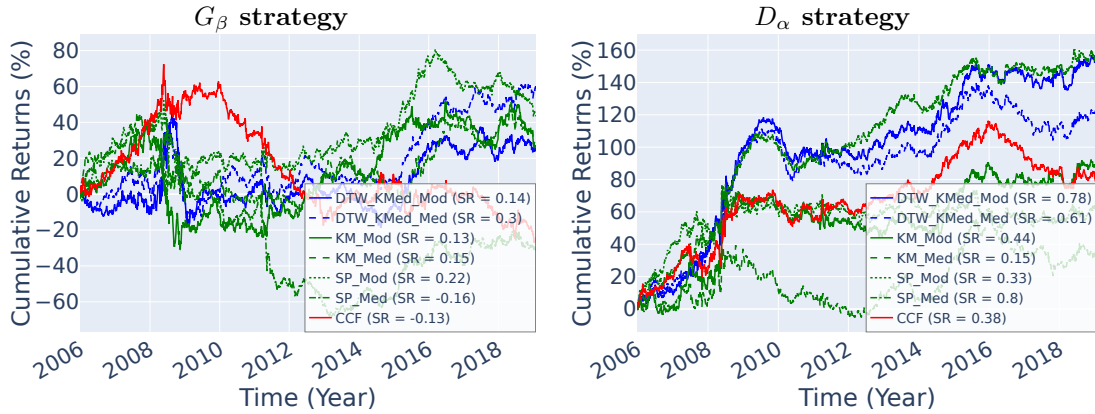


Figure 11: ETF data set: cumulative PnL for G_β strategy (left) and D_α strategy (right) - rescaled to target volatility. The experiment has been set with the values $p = 7$, $\delta = 7$, $\alpha = 0.25$, and $K = 5$.

G_β strategy	Benchmark				Proposed		
	CCF	KM_Mod	KM_Med	SP_Mod	SP_Med	DTW_KMod_Mod	DTW_KMod_Med
E[Returns]	-0.019	0.02	0.022	0.033	-0.024	0.021	0.045
Volatility	0.15	0.15	0.15	0.15	0.15	0.15	0.15
Downside deviation	0.116	0.115	0.116	0.113	0.123	0.111	0.115
Maximum drawdown	-0.668	-0.525	-0.465	-0.38	-0.653	-0.507	-0.428
Sortino ratio	-0.165	0.176	0.188	0.294	-0.192	0.186	0.394
Calmar ratio	-0.029	0.038	0.047	0.088	-0.036	0.041	0.106
Hit rate	0.492	0.512	0.499	0.509	0.509	0.512	0.513
Avg. profit / avg. loss	1.006	0.978	1.034	1.009	0.935	0.98	1.005
PnL per trade	-0.76	0.8	0.87	1.325	-0.939	0.818	1.799
Sharpe ratio	-0.128	0.134	0.146	0.223	-0.158	0.137	0.302
P-value	0.644	0.628	0.598	0.421	0.568	0.619	0.275

Table 5: ETF data set: performance metrics for G_β strategy - rescaled to target volatility. The experiment has been set with the values $p = 7$, $\delta = 7$, $\alpha = 0.25$, and $K = 5$.

G_β strategy	Benchmark				Proposed		
	CCF	KM_Mod	KM_Med	SP_Mod	SP_Med	DTW_KMod_Mod	DTW_KMod_Med
E[Returns]	0.056	0.065	0.022	0.05	0.121	0.117	0.091
Volatility	0.15	0.15	0.15	0.15	0.15	0.15	0.15
Downside deviation	0.097	0.097	0.105	0.104	0.098	0.093	0.095
Maximum drawdown	-0.362	-0.267	-0.385	-0.298	-0.22	-0.256	-0.31
Sortino ratio	0.581	0.676	0.213	0.474	1.236	1.257	0.955
Calmar ratio	0.156	0.245	0.058	0.166	0.548	0.456	0.293
Hit rate	0.504	0.502	0.5	0.508	0.513	0.521	0.517
Avg. profit / avg. loss	1.056	1.077	1.027	1.03	1.097	1.056	1.039
PnL per trade	2.234	2.591	0.889	1.965	4.784	4.635	3.608
Sharpe ratio	0.375	0.435	0.149	0.33	0.804	0.779	0.606
P-value	0.169	0.105	0.588	0.229	0.003	0.004	0.026

Table 6: ETF data set: performance metrics for D_α strategy - rescaled to target volatility. The experiment has been set with the values $p = 7$, $\delta = 7$, $\alpha = 0.25$, and $K = 5$.

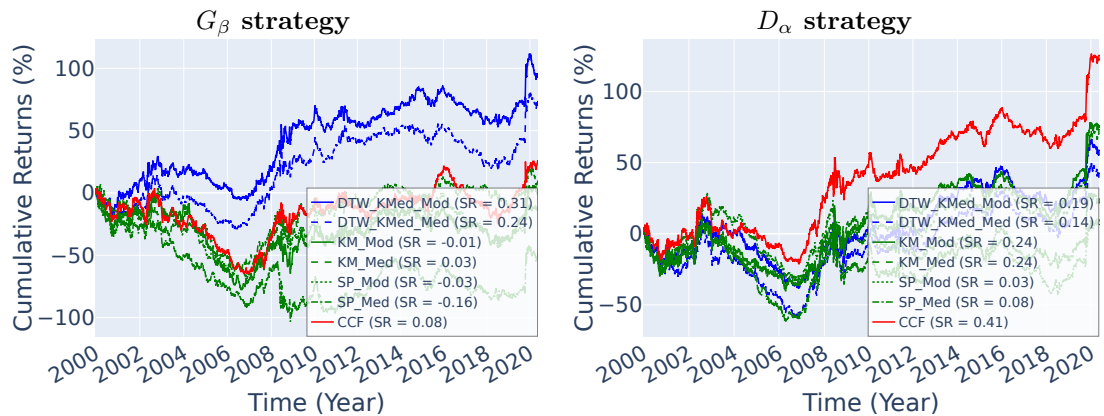


Figure 12: Futures data set: cumulative PnL for G_β strategy (left) and D_α strategy (right) - rescaled to target volatility. The experiment has been set with the values $p = 7$, $\delta = 7$, $\alpha = 0.25$, and $K = 5$.

G_β strategy	Benchmark					Proposed	
	CCF	KM.Mod	KM.Med	SP.Mod	SP.Med	DTW_KMod_Mod	DTW_KMod_Med
E[Returns]	0.013	-0.001	0.004	-0.005	-0.024	0.047	0.036
Volatility	0.15	0.15	0.15	0.15	0.15	0.15	0.15
Downside deviation	0.104	0.102	0.103	0.107	0.109	0.103	0.104
Maximum drawdown	-0.535	-0.587	-0.538	-0.544	-0.698	-0.316	-0.376
Sortino ratio	0.121	-0.01	0.042	-0.049	-0.217	0.453	0.347
Calmar ratio	0.024	-0.002	0.008	-0.01	-0.034	0.147	0.096
Hit rate	0.502	0.498	0.494	0.497	0.497	0.506	0.505
Avg. profit / avg. loss	1.007	1.008	1.028	1.006	0.984	1.033	1.023
PnL per trade	0.499	-0.039	0.173	-0.206	-0.94	1.848	1.427
Sharpe ratio	0.084	-0.007	0.029	-0.035	-0.158	0.31	0.24
P-value	0.705	0.976	0.896	0.876	0.476	0.159	0.278

Table 7: Futures data set: performance metrics for G_β strategy - rescaled to target volatility. The experiment has been set with the values $p = 7$, $\delta = 7$, $\alpha = 0.25$, and $K = 5$.

G_β strategy	Benchmark					Proposed	
	CCF	KM.Mod	KM.Med	SP.Mod	SP.Med	DTW_KMod_Mod	DTW_KMod_Med
E[Returns]	0.061	0.036	0.036	0.005	0.012	0.029	0.021
Volatility	0.15	0.15	0.15	0.15	0.15	0.15	0.15
Downside deviation	0.107	0.108	0.108	0.11	0.105	0.107	0.107
Maximum drawdown	-0.393	-0.412	-0.404	-0.581	-0.524	-0.424	-0.502
Sortino ratio	0.574	0.337	0.331	0.042	0.112	0.269	0.193
Calmar ratio	0.156	0.088	0.089	0.008	0.022	0.068	0.041
Hit rate	0.511	0.502	0.499	0.491	0.496	0.498	0.501
Avg. profit / avg. loss	1.032	1.038	1.05	1.042	1.032	1.042	1.022
PnL per trade	2.439	1.445	1.424	0.183	0.468	1.139	0.822
Sharpe ratio	0.41	0.243	0.239	0.031	0.079	0.191	0.138
P-value	0.064	0.272	0.28	0.889	0.723	0.387	0.533

Table 8: Futures data set: performance metrics for D_α strategy - rescaled to target volatility. The experiment has been set with the values $p = 7$, $\delta = 7$, $\alpha = 0.25$, and $K = 5$.

7 Robustness analysis

We test the robustness of the DTW_KMod_Mod and DTW_KMod_Med by conducting experiments with different numbers of clusters K . Specifically, for the equity data set, we consider $K = \{5, 10, 15, 20\}$. In Table 9, we observe that the performance of both algorithms does not change significantly while maintaining a high SR. It is worth noting that the P-values are almost all lower than 0.05, indicating that all the results are statistically significant in our experiments.

Table 10 presents the performance of the DTW_KMod_Mod and DTW_KMod_Med tested on the ETF data set. Due to the smaller cross-section for this data set, we only consider the K values of 5 and 10. Both algorithms demonstrate fairly good performance for high alpha in the D_α strategy.

Table 11 presents the performance of the DTW_KMod_Mod and DTW_KMod_Med on the futures data set, with K ranging from 5 to 20 in increments of 5. It is observed that for this data set, the SR for the D_α strategy tends to be more sensitive to changes in K , and achieving profitability becomes challenging.

DTW_KMod_Mod	G_β strategy				D_α strategy				
	K	5	10	15	20	5	10	15	20
E[Returns]		0.109	0.098	0.098	0.096	0.128	0.106	0.114	0.101
Volatility		0.15	0.15	0.15	0.15	0.15	0.15	0.15	0.15
Downside deviation		0.106	0.107	0.108	0.108	0.103	0.105	0.105	0.105
Maximum drawdown		-0.205	-0.192	-0.198	-0.235	-0.276	-0.27	-0.221	-0.272
Sortino ratio		1.026	0.92	0.908	0.891	1.238	1.007	1.084	0.961
Calmar ratio		0.531	0.512	0.497	0.408	0.463	0.392	0.514	0.372
Hit rate		0.514	0.512	0.516	0.514	0.52	0.519	0.522	0.519
Avg. profit / avg. loss		1.08	1.075	1.058	1.066	1.078	1.051	1.05	1.044
PnL per trade		4.317	3.9	3.906	3.805	5.073	4.201	4.511	4.012
Sharpe ratio		0.725	0.655	0.656	0.639	0.852	0.706	0.758	0.674
P-value		0.001	0.004	0.004	0.005	0	0.002	0.001	0.003

DTW_KMod_Med	G_β strategy				D_α strategy				
	K	5	10	15	20	5	10	15	20
E[Returns]		0.115	0.097	0.083	0.092	0.14	0.116	0.099	0.112
Volatility		0.15	0.15	0.15	0.15	0.15	0.15	0.15	0.15
Downside deviation		0.107	0.107	0.109	0.109	0.102	0.104	0.105	0.104
Maximum drawdown		-0.188	-0.197	-0.226	-0.21	-0.297	-0.226	-0.241	-0.274
Sortino ratio		1.084	0.907	0.76	0.844	1.376	1.112	0.946	1.083
Calmar ratio		0.614	0.493	0.367	0.437	0.472	0.513	0.413	0.41
Hit rate		0.512	0.513	0.509	0.513	0.523	0.519	0.514	0.517
Avg. profit / avg. loss		1.1	1.069	1.07	1.065	1.078	1.067	1.067	1.068
PnL per trade		4.581	3.851	3.293	3.646	5.557	4.596	3.948	4.459
Sharpe ratio		0.77	0.647	0.553	0.612	0.934	0.772	0.663	0.749
P-value		0.001	0.004	0.015	0.007	0	0.001	0.003	0.001

Table 9: Equity data set: robustness analysis for K - rescaled to target volatility. The experiment has been set with the values $p = 7$, and $\delta = 7$.

DTW_KMod_Mod	G_β strategy		D_α strategy	
	5	10	5	10
K				
E[Returns]	0.021	0.058	0.117	0.07
Volatility	0.15	0.15	0.15	0.15
Downside deviation	0.111	0.116	0.093	0.098
Maximum drawdown	-0.507	-0.353	-0.256	-0.321
Sortino ratio	0.186	0.505	1.257	0.715
Calmar ratio	0.041	0.166	0.456	0.219
Hit rate	0.512	0.506	0.521	0.505
Avg. profit / avg. loss	0.98	1.059	1.056	1.067
PnL per trade	0.818	2.321	4.635	2.783
Sharpe ratio	0.137	0.39	0.779	0.468
P-value	0.619	0.161	0.004	0.088

DTW_KMod_Med	G_β strategy		D_α strategy	
	5	10	5	10
K				
E[Returns]	0.045	0.063	0.091	0.061
Volatility	0.15	0.15	0.15	0.15
Downside deviation	0.115	0.113	0.095	0.098
Maximum drawdown	-0.428	-0.415	-0.31	-0.388
Sortino ratio	0.394	0.561	0.955	0.621
Calmar ratio	0.106	0.153	0.293	0.157
Hit rate	0.513	0.508	0.517	0.507
Avg. profit / avg. loss	1.005	1.054	1.039	1.045
PnL per trade	1.799	2.514	3.608	2.413
Sharpe ratio	0.302	0.422	0.606	0.405
P-value	0.275	0.128	0.026	0.14

Table 10: ETF data set: robustness analysis for K - rescaled to target volatility. The experiment has been set with the values $p = 7$, and $\delta = 7$.

DTW_KMod_Mod	G_β strategy				D_α strategy			
	5	10	15	20	5	10	15	20
K								
E[Returns]	0.047	0.051	0.064	0.055	0.029	0.042	0.048	0.04
Volatility	0.15	0.15	0.15	0.15	0.15	0.15	0.15	0.15
Downside deviation	0.103	0.102	0.103	0.104	0.107	0.105	0.105	0.105
Maximum drawdown	-0.316	-0.412	-0.421	-0.338	-0.424	-0.468	-0.459	-0.455
Sortino ratio	0.453	0.496	0.618	0.528	0.269	0.395	0.457	0.378
Calmar ratio	0.147	0.123	0.152	0.163	0.068	0.089	0.105	0.087
Hit rate	0.506	0.5	0.501	0.508	0.498	0.5	0.5	0.499
Avg. profit / avg. loss	1.033	1.065	1.08	1.04	1.042	1.05	1.058	1.055
PnL per trade	1.848	2.015	2.534	2.19	1.139	1.649	1.908	1.577
Sharpe ratio	0.31	0.338	0.426	0.368	0.191	0.277	0.321	0.265
P-value	0.159	0.124	0.053	0.095	0.387	0.21	0.147	0.231

DTW_KMod_Med	G_β strategy				D_α strategy			
	5	10	15	20	5	10	15	20
K								
E[Returns]	0.036	0.05	0.061	0.055	0.021	0.033	0.053	0.039
Volatility	0.15	0.15	0.15	0.15	0.15	0.15	0.15	0.15
Downside deviation	0.104	0.104	0.105	0.106	0.107	0.105	0.106	0.105
Maximum drawdown	-0.376	-0.376	-0.428	-0.365	-0.502	-0.465	-0.475	-0.479
Sortino ratio	0.347	0.48	0.583	0.521	0.193	0.313	0.505	0.374
Calmar ratio	0.096	0.133	0.143	0.151	0.041	0.071	0.112	0.082
Hit rate	0.505	0.502	0.505	0.506	0.501	0.499	0.504	0.499
Avg. profit / avg. loss	1.023	1.055	1.057	1.048	1.022	1.045	1.052	1.054
PnL per trade	1.427	1.978	2.436	2.184	0.822	1.305	2.115	1.556
Sharpe ratio	0.24	0.332	0.409	0.367	0.138	0.219	0.355	0.261
P-value	0.278	0.132	0.063	0.096	0.533	0.321	0.108	0.237

Table 11: Futures data set: robustness analysis for K - rescaled to target volatility. The experiment has been set with the values $p = 7$, and $\delta = 7$.

8 CONCLUSION AND FUTURE WORK

In this study, we introduce a Dynamic Time Warping (DTW) based approach for robustly detecting lead-lag relationships in high-dimensional multivariate time series, with a specific focus on lagged multi-factor models. Our proposed algorithms show promising Sharpe Ratios when applied to financial data sets, indicating their potential economic benefits compared to the benchmark.

To enhance the methodology further, a possible future direction could involve exploring dynamic selection of the number of clusters K . Additionally, another interesting direction would be to delve into the more intricate mixed membership model described in Section 3, which poses a more challenging task. Investigating intraday lead-lag relationships using, for example, minutely data, could be another fruitful area of research.

References

- [1] John Aach and George M Church. “Aligning gene expression time series with time warping algorithms”. In: *Bioinformatics* 17.6 (2001), pp. 495–508.
- [2] Jakob Albers et al. “Fragmentation, price formation and cross-impact in bitcoin markets”. In: *Applied Mathematical Finance* 28.5 (2021), pp. 395–448.
- [3] Qi Jin Álvaro Cartea Mihai Cucuringu. “Correlation matrix clustering for statistical arbitrage portfolios”. 2023.
- [4] David H Bailey and Marcos Lopez De Prado. “The deflated Sharpe ratio: correcting for selection bias, backtest overfitting, and non-normality”. In: *The Journal of Portfolio Management* 40.5 (2014), pp. 94–107.
- [5] Afonso S Bandeira et al. “Multireference alignment using semidefinite programming”. In: *Proceedings of the 5th conference on Innovations in theoretical computer science*. 2014, pp. 459–470.
- [6] Richard Bellman and Robert Kalaba. “On adaptive control processes”. In: *IRE Transactions on Automatic Control* 4.2 (1959), pp. 1–9.
- [7] Stefanos Bennett, Mihai Cucuringu, and Gesine Reinert. “Lead-lag detection and network clustering for multivariate time series with an application to the US equity market”. In: *Machine Learning* 111.12 (2022), pp. 4497–4538.
- [8] Donald J Berndt and James Clifford. “Using dynamic time warping to find patterns in time series”. In: *Proceedings of the 3rd international conference on knowledge discovery and data mining*. 1994, pp. 359–370.
- [9] Giuseppe Buccheri, Fulvio Corsi, and Stefano Peluso. “High-frequency lead-lag effects and cross-asset linkages: a multi-asset lagged adjustment model”. In: *Journal of Business & Economic Statistics* 39.3 (2021), pp. 605–621.
- [10] Jay Cao, Jacky Chen, and John Hull. “A neural network approach to understanding implied volatility movements”. In: *Quantitative Finance* 20.9 (2020), pp. 1405–1413.

- [11] Alvaro Cartea, Ryan Donnelly, and Sebastian Jaimungal. “Enhancing trading strategies with order book signals”. In: *Applied Mathematical Finance* 25.1 (2018), pp. 1–35.
- [12] Rama Cont. “Empirical properties of asset returns: stylized facts and statistical issues”. In: *Quantitative finance* 1.2 (2001), p. 223.
- [13] Yan Cui, Jun Yang, and Zhou Zhou. “State-domain change point detection for nonlinear time series regression”. In: *Journal of Econometrics* (2021).
- [14] Giovanni De Luca and Federica Pizzolante. “Detecting Leaders Country from Road Transport Emission Time-Series”. In: *Environments* 8.3 (2021), p. 18.
- [15] Felix Drinkall, Stefan Zohren, and Janet B Pierrehumbert. “Forecasting COVID-19 Caseloads Using Unsupervised Embedding Clusters of Social Media Posts”. In: *arXiv:2205.10408* (2022).
- [16] Dariu M Gavrilă, Larry S Davis, et al. “Towards 3-d model-based tracking and recognition of human movement: a multi-view approach”. In: *International workshop on automatic face-and gesture-recognition*. Vol. 3. Citeseer. 1995, pp. 272–277.
- [17] David F Gleich and Lek-heng Lim. “Rank aggregation via nuclear norm minimization”. In: *Proceedings of the 17th ACM SIGKDD international conference on Knowledge discovery and data mining*. 2011, pp. 60–68.
- [18] Kartikay Gupta and Niladri Chatterjee. “Examining lead-lag relationships in-depth, with focus on FX market as Covid-19 crises unfolds”. In: *arXiv:2004.10560* (2020).
- [19] Clint Howard, Talis J Putninš, and Vitali Alexeev. “To lead or to lag? Measuring asynchronicity in financial time-series using dynamic time warping”. In: (2022).
- [20] Peter J Huber. “Pairwise comparison and ranking: optimum properties of the row sum procedure”. In: *The annals of mathematical statistics* (1963), pp. 511–520.
- [21] Katsuya Ito and Ryuta Sakemoto. “Direct estimation of lead-lag relationships using multinomial dynamic time warping”. In: *Asia-Pacific Financial Markets* 27.3 (2020), pp. 325–342.
- [22] Narasimhan Jegadeesh, Jiang Luo, et al. “Momentum and short-term reversals: theory and evidence”. In: *Nanyang Business School Research Paper* 22-13 (2022).
- [23] Narasimhan Jegadeesh and Sheridan Titman. “Profitability of momentum strategies: An evaluation of alternative explanations”. In: *The Journal of finance* 56.2 (2001), pp. 699–720.
- [24] Eamonn Keogh and Chotirat Ann Ratanamahatana. “Exact indexing of dynamic time warping”. In: *Knowledge and information systems* 7 (2005), pp. 358–386.
- [25] Oliver Ledoit and Michael Wolf. “Robust performance hypothesis testing with the Sharpe ratio”. In: *Journal of Empirical Finance* 15.5 (2008), pp. 850–859.
- [26] Yongli Li et al. “Dynamic patterns of daily lead-lag networks in stock markets”. In: *Quantitative Finance* 21.12 (2021), pp. 2055–2068.
- [27] Bryan Lim, Stefan Zohren, and Stephen Roberts. “Enhancing time-series momentum strategies using deep neural networks”. In: *The Journal of Financial Data Science* 1.4 (2019), pp. 19–38.

- [28] Tom Liu, Stephen Roberts, and Stefan Zohren. “Deep Inception Networks: A General End-to-End Framework for Multi-asset Quantitative Strategies”. In: *arXiv preprint arXiv:2307.05522* (2023).
- [29] Tom Liu and Stefan Zohren. “Multi-Factor Inception: What to Do with All of These Features?” In: *arXiv preprint arXiv:2307.13832* (2023).
- [30] Yutong Lu, Gesine Reinert, and Mihai Cucuringu. “Co-trading networks for modeling dynamic interdependency structures and estimating high-dimensional covariances in US equity markets”. In: *arXiv:2302.09382* (2023).
- [31] Yutong Lu, Gesine Reinert, and Mihai Cucuringu. “Trade co-occurrence, trade flow decomposition, and conditional order imbalance in equity markets”. In: *arXiv:2209.10334* (2022).
- [32] Wannes Meert et al. *DTAIDistance*. Version v2.3.10. If you use this software, please cite it as below. Aug. 2020. DOI: [10.5281/zenodo.7158824](https://doi.org/10.5281/zenodo.7158824). URL: <https://doi.org/10.5281/zenodo.7158824>.
- [33] Nikolas Michael, Mihai Cucuringu, and Sam Howison. “Option Volume Imbalance as a predictor for equity market returns”. In: *arXiv:2201.09319* (2022).
- [34] Deborah Miori and Mihai Cucuringu. “Returns-Driven Macro Regimes and Characteristic Lead-Lag Behaviour between Asset Classes”. In: *arXiv:2209.00268* (2022).
- [35] Daniel Poh, Stephen Roberts, and Stefan Zohren. “Transfer ranking in finance: applications to cross-sectional momentum with data scarcity”. In: *arXiv:2208.09968* (2022).
- [36] Stephen Roberts, Xiaowen Dong, Stefan Zohren, et al. “Network Momentum across Asset Classes”. In: *arXiv preprint arXiv:2308.11294* (2023).
- [37] Jakob Runge et al. “Detecting and quantifying causal associations in large nonlinear time series datasets”. In: *Science advances* 5.11 (2019), eaau4996.
- [38] Matthew D Schmill, Tim Oates, and Paul R Cohen. “Learned models for continuous planning.” In: *AISTATS*. Citeseer. 1999.
- [39] Pavel Senin. “Dynamic time warping algorithm review”. In: *Information and Computer Science Department University of Hawaii at Manoa Honolulu, USA* 855.1-23 (2008), p. 40.
- [40] Alik Sokolov et al. “Assessing the Impact of Sustainability on Fund Flows: An Excess Information Approach and US-Based Case Study”. In: *The Journal of Impact and ESG Investing* (2022).
- [41] Johannes Stübinger and Dominik Walter. “Using multi-dimensional dynamic time warping to identify time-varying lead-lag relationships”. In: *Sensors* 22.18 (2022), p. 6884.
- [42] Wee Ling Tan, Stephen Roberts, and Stefan Zohren. “Spatio-Temporal Momentum: Jointly Learning Time-Series and Cross-Sectional Strategies”. In: *arXiv:2302.10175* (2023).
- [43] Konstantinos Tolikas. “The lead-lag relation between the stock and the bond markets”. In: *The European Journal of Finance* 24.10 (2018), pp. 849–866.

- [44] Milena Vuletić, Felix Prenzel, and Mihai Cucuringu. “Fin-GAN: Forecasting and Classifying Financial Time Series via Generative Adversarial Networks”. In: *Available at SSRN 4328302* (2023).
- [45] Kieran Wood, Sven Giegerich, et al. “Trading with the Momentum Transformer: An Intelligent and Interpretable Architecture”. In: *arXiv:2112.08534* (2021).
- [46] Kieran Wood, Stephen Roberts, and Stefan Zohren. “Slow momentum with fast reversion: A trading strategy using deep learning and changepoint detection”. In: *arXiv:2105.13727* (2021).
- [47] Kieran Wood, Stephen Roberts, and Stefan Zohren. “Slow momentum with fast reversion: A trading strategy using deep learning and changepoint detection”. In: *The Journal of Financial Data Science* 4.1 (2022), pp. 111–129.
- [48] Di Wu et al. “Detecting leaders from correlated time series”. In: *International Conference on Database Systems for Advanced Applications*. Springer. 2010, pp. 352–367.
- [49] Can-Zhong Yao and Hong-Yu Li. “Time-varying lead–lag structure between investor sentiment and stock market”. In: *The North American Journal of Economics and Finance* 52 (2020), p. 101148.
- [50] Yichi Zhang, Mihai Cucuringu, Alexander Shestopaloff, et al. *Supplemental Material: Dynamic Time Warping for Lead-Lag Relationships in Lagged Multi-Factor Models*. Mendeley Data. Version V1. 2023. DOI: [10.17632/wpszpcftg2.1](https://doi.org/10.17632/wpszpcftg2.1).
- [51] Yichi Zhang, Mihai Cucuringu, Alexander Y Shestopaloff, et al. “Robust Detection of Lead-Lag Relationships in Lagged Multi-Factor Models”. In: *arXiv:2305.06704* (2023).
- [52] Stefan Zohren, Stephen Roberts, Xiaowen Dong, et al. “Learning to Learn Financial Networks for Optimising Momentum Strategies”. In: *arXiv preprint arXiv:2308.12212* (2023).

A Appendix

A.1 Performance metrics

The cumulative PnL is the sum of daily PnL across all trading days

$$\text{Cumulative PnL} = \sum \text{PnL}_{\text{rescaled}}. \quad (16)$$

The annualized expected excess return ($E[\text{Returns}]$) is a measure of the excess return earned by an investment over a benchmark index during a one-year period. This value can be calculated by

$$E[\text{Returns}] = \text{AVG}(\text{PnL}_{\text{rescaled}}) \cdot 252. \quad (17)$$

The annualized volatility measures the one-year risk associated with an investment

$$\text{Volatility} = \text{STD}(\text{PnL}_{\text{rescaled}}) \cdot \sqrt{252}. \quad (18)$$

Additionally, we calculate downside deviation and maximum drawdown to measure downside risk. The Sortino ratio is often preferred by investors more concerned with downside risk than overall risk or volatility. It is derived by

$$\text{Sortino ratio} = \frac{E[\text{Returns}]}{\text{downside deviation}}. \quad (19)$$

The Calmar ratio is frequently utilized by investors with a focus on long-term risk and downside protection. A higher Calmar ratio signifies that the strategy has produced superior returns relative to its maximum drawdown, while a lower Calmar ratio suggests underperformance considering the level of risk taken. This ratio is calculated by

$$\text{Calmar ratio} = \frac{E[\text{Returns}]}{\text{maximum drawdown}}. \quad (20)$$

The hit rate, also known as the win rate or success rate, measures the percentage of successful trades made by the strategy. It is defined as

$$\text{Hit rate} = \frac{|\text{PnL}_{\text{rescaled}}^+|}{|\text{PnL}_{\text{rescaled}}|}, \quad (21)$$

where $|\text{PnL}_{\text{rescaled}}^+|$ is the number of profitable trades, and $|\text{PnL}_{\text{rescaled}}|$ is the total number of trades.

The average profit / average loss (avg. profit / avg. loss) ratio measures the strategy's average profit size relative to its average loss size

$$\text{Avg. profit / avg. loss} = \frac{\text{AVG}(\text{PnL}_{\text{rescaled}}^+)}{\text{AVG}(\text{PnL}_{\text{rescaled}}^-)}, \quad (22)$$

where $\text{AVG}(\text{PnL}_{\text{rescaled}}^+)$ is the average profit per trade, and $\text{AVG}(\text{PnL}_{\text{rescaled}}^-)$ is the average loss

per trade.

The PnL per trade illustrates the amount earned by the strategy, in basis points, for each basket of G_β or D_α traded in the markets (excluding transaction costs). It is given by

$$\text{PnL per trade} = \text{AVG}(\text{PnL}_{\text{rescaled}}) \cdot 10^4, \quad (23)$$

where we assume that the strategy trades the same amount of notional every day (i.e., a constant unit bet size is used every trading day).

We also compute the annualized Sharpe ratio to quantify the profit gained per unit of risk taken

$$\text{Sharpe ratio} = \frac{\text{AVG}(\text{PnL}_{\text{rescaled}})}{\text{STD}(\text{PnL}_{\text{rescaled}})} \cdot \sqrt{252}. \quad (24)$$

It is important to assess the statistical significance of Sharpe ratio when back-testing a sample of hypothetical strategies [Bailey and De Prado (2014), Ledoit and Wolf (2008), Michael, Cucuringu, and Howison (2022)]. We use a test with the null hypothesis $H_0 : \text{Sharpe ratio} = 0$, and implement the method proposed by [Bailey and De Prado (2014)] to compute the test statistic

$$\frac{(\text{Sharpe ratio}) \cdot \sqrt{T-1}}{\sqrt{1 - \gamma_1 \cdot (\text{Sharpe ratio}) + (\gamma_2 - 1) \cdot (\text{Sharpe ratio})^2/4}}, \quad (25)$$

where the Sharpe ratio is what we are testing, T represents the length of the sample, and γ_1 and γ_2 are the skewness and kurtosis of the returns distribution for the selected strategy, respectively. Under the null hypothesis, this test statistic is assumed to follow a standard normal distribution.

To assess the predictive performance of our algorithm, we create a straightforward trading strategy. If this strategy proves profitable with a statistically significant Sharpe ratio, it signifies our ability to leverage the discovered lead-lag relationships for the prediction task.

A.2 Synthetic data experiments

Figure 13 presents the results of synthetic data experiments for the G_β strategy (left) and D_α strategy (right). In both the Homogeneous Setting and Heterogeneous Setting, the SR of all algorithms consistently increased with the number of days. Additionally, when the noise level increased from 1 to 2, the SR of the algorithms was not significantly affected. In particular, DTW_KMed_Mod and DTW_KMed_Med outperform other algorithms in the G_β strategy.

In Figures 14 and 15, as the number of days increases, we observe a consistent pattern for G_β and D_α in both the G_β strategy (left) and D_α strategy (right), regardless of whether it is in the homogeneous setting or heterogeneous setting. Although there is a slight deviation as the level of noise increases from 1 to 2, overall, the results of both strategies align with the experimental expectations, primarily due to the structure of the lag matrix L .

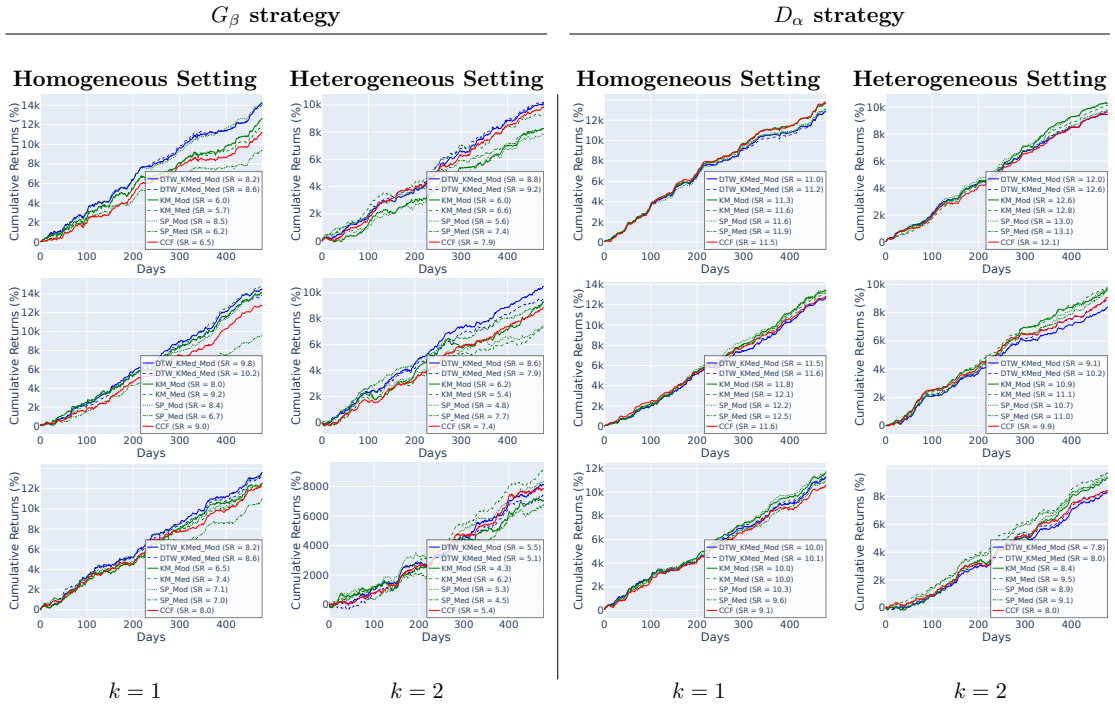


Figure 13: Left: G_β strategy. Right: D_α strategy. The synthetic data set cumulative PnL experiment has been set with the values $n = 120$, $p = 1$, $\delta = 1$, and $\alpha = 0.25$. From top panel to bottom panel, low noise $\sigma = 1$, Medium noise $\sigma = 1.5$, and high noise $\sigma = 2$.

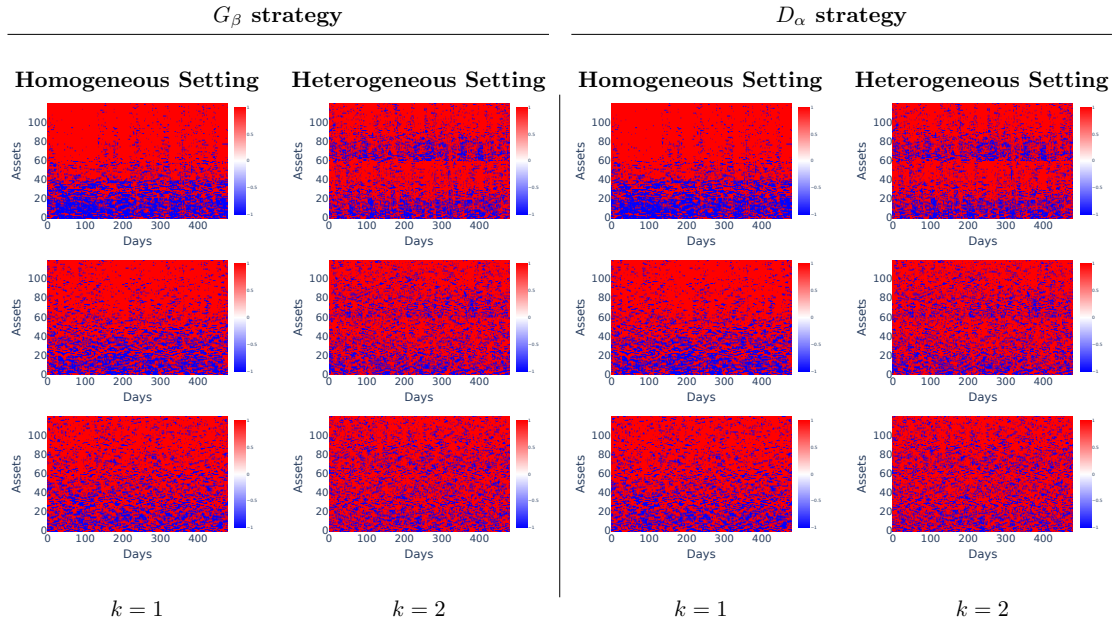


Figure 14: DTW_KMod_Mod: Left: G_β strategy. Right: D_α strategy. G_β are colored in blue, and D_α are colored in red. The synthetic data set has been set with the values $n = 120$, $p = 1$, $\delta = 1$, and $\alpha = 0.25$. From top panel to bottom panel, low noise $\sigma = 1$, Medium noise $\sigma = 1.5$, and high noise $\sigma = 2$.

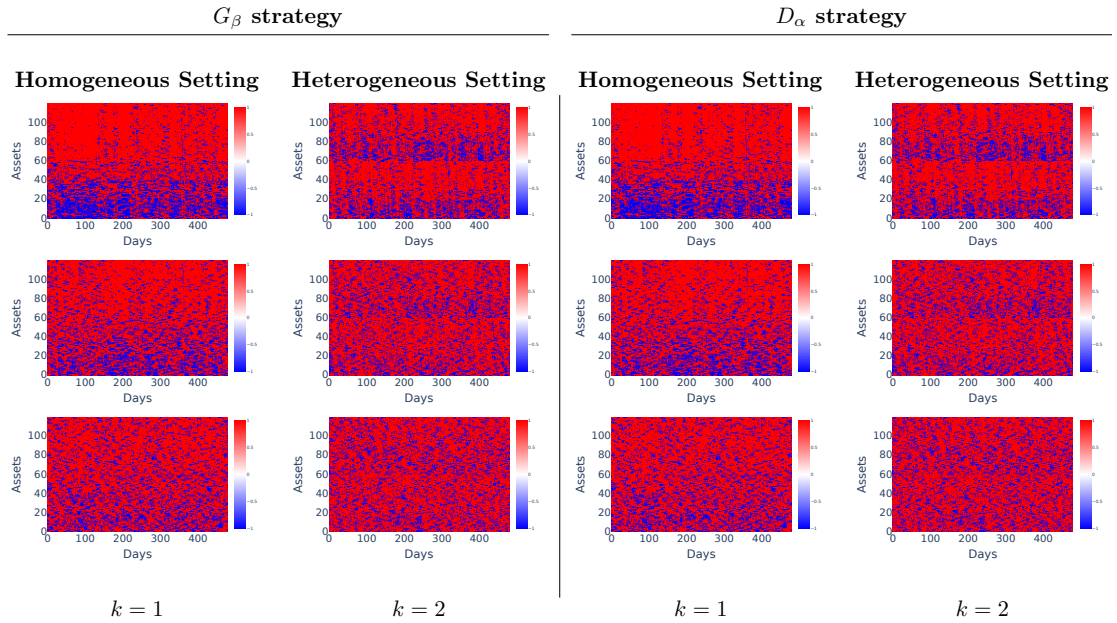


Figure 15: DTW_KMod_Med: Left: G_β strategy. Right: D_α strategy. G_β are colored in blue, and D_α are colored in red. The synthetic data set has been set with the values $n = 120$, $p = 1$, $\delta = 1$, and $\alpha = 0.25$. From top panel to bottom panel, low noise $\sigma = 1$, Medium noise $\sigma = 1.5$, and high noise $\sigma = 2$.

A.3 Futures data set details

Tables [12, 13, 14, 15, 16, 17, 18, 19] show the futures contracts we used and its description from the Pinnacle Data Corp CLC Database. The data is based on ratio-adjusted methods, which removes the contract-to-contract gap, yet it will not go negative as it reduces the size of the price bars if they go lower and increases them if they go higher.

Table 12: Grains

Identifier	Description
KW	WHEAT, KC
MW	WHEAT, MINN
NR	ROUGH RICE
W_	WHEAT, CBOT
ZC	CORN, Electronic
ZL	SOYBEAN OIL, Electronic
ZM	SOYBEAN MEAL, Electronic
ZO	OATS, Electronic
ZR	ROUGH RICE, Electronic
ZS	SOYBEANS, Electronic
ZW	WHEAT, Electronic

Table 13: Meats

Identifier	Description
DA	MILK III, Comp.
ZF	FEEDER CATTLE, Electronic
ZT	LIVE CATTLE, Electronic
ZZ	LEAN HOGS, Electronic

Table 14: Wood fibre

Identifier	Description
LB	LUMBER

Table 15: Metals

Identifier	Description
ZG	GOLD, Electronic
ZI	SILVER, Electronic
ZP	PLATINUM, electronic
ZA	PALLADIUM, electronic
ZK	COPPER, electronic

Table 16: Indexes

Identifier	Description
AX	GERMAN DAX INDEX
CA	CAC40 INDEX
DX	US DOLLAR INDEX
EN	NASDAQ, MINI
ES	S & P 500, MINI
GI	GOLDMAN SAKS C. I.
LX	FTSE 100 INDEX
MD	S & P 400 (Mini electronic)
NK	NIKKEI INDEX
SC	S & P 500, composite

Table 17: Bonds

Identifier	Description
DT	EURO BOND (BUND)
FB	T-NOTE, 5yr composite
GS	GILT, LONG BOND
SS	STERLING, SHORT
TY	T-NOTE, 10yr composite
TU	T-NOTES, 2yr composite
US	T-BONDS, composite
UB	EURO BOBL
UZ	EURO SCHATZ

Table 18: Currency

Identifier	Description
AN	AUSTRALIAN \$\$ composite
BN	BRITISH POUND, composite
CN	CANADIAN \$\$ composite
EC	EURODOLLAR, composite
FN	EURO, composite
JN	JAPANESE YEN, composite
MP	MEXICAN PESO
SN	SWISS FRANC, composite

Table 19: Oils

Identifier	Description
ZB	RBOB, Electronic
ZH	HEATING OIL, electronic
ZN	NATURAL GAS, electronic
ZU	CRUDE OIL, Electronic